Electrical Power and Energy Systems 104 (2019) 603–614

Contents lists available at ScienceDirect

Electrical Power and Energy Systems

journal homepage: www.elsevier.com/locate/ijepes

Load frequency control strategy via fractional-order controller and reduced-order modeling

Sahaj Saxena*

Electrical and Instrumentation Engineering Department, Thapar Institute of Engineering and Technology, Patiala 147004, India

A R T I C L E I N F O

Keywords:
Fractional-order filter
Internal model control
Load frequency control
PID tuning
Reduced model

A B S T R A C T

This paper proposes a simple approach to design fractional-order (FO) controller via internal model control (IMC) technique for load frequency control (LFC) problem in power systems. The proposed scheme utilizes the concept of CRONE principle, model-order reduction and FO filter in IMC framework to derive a robust controller. Initially, the scheme is applied to single-area power system and then extended to two-area interconnected system. The turbines considered are non-reheated, reheated and hydro type; and physical constraints of turbine and governor are also taken into account to validate the applicability in more realistic environment. Simulation results show that it can bring improved disturbance rejection performance in nominal condition as well as in presence of uncertainties and constraints in plant parameters.

1. Introduction

Power system control is one of the most challenging task in control engineering because the total generated power should balance the total load in presence of numerous electrical machines such as generating units, protection devices, controller loops and power transmission lines that generally spread in large geographical areas. Essentially, there would be performance deterioration in the form of frequency fluctuations, voltage instability, constant but unexpected load change, operational limits, rotor angle instability, economy in operation, and physical and environmental disturbances. Therefore, these discrepancies must be eliminated for satisfactory operation of power system.

Among the various power system control strategies [1], LFC deals with the regulation of frequency fluctuations,*i.e.*, frequency should remain nearly constant in all control areas. In short, the LFC adjusts the load reference point against the variation of the load changes in order to keep the system frequency and tie-line power as closed to the prescribed values as possible. The main objectives of LFC are to: 1) maintain zero steady state error for frequency and tie-line power deviations, 2) reject sudden load disturbance, 3) attain optimal transient behavior under prescribed overshoot, settling time and error tolerance, 4) provide robust performance in presence of modeling uncertainties and nonlinearities, 5) establish better security margin of system in sense of stable frequency regulation, and less computing power [2–4]. Thus, LFC can be treated as an objective optimization and robust control problem. In view of this various LFC strategies have been developed using optimal, robust, adaptive and intelligent control perspectives [5–7].

These days FO control scheme has received great attention among the control practitioners due to improved control performance especially for the systems working in uncertain environment, and exact modeling of complex systems [8,9]. The FO system and control schemes are generally better than their integer-order (IO) counterparts. As a result, a few fractional-order PID (FO-PID) control methodologies have also been introduced for LFC problem. The first FO-PID scheme was presented by Alomoush [10] in which LFC has been considered as a constrained optimization problem for two-area power systems. The integral error criterion particularly *ITAE* was selected as an optimization function to evaluate PID parameters. In [11], the stability boundary locus method was employed to search the stabilizing FO-PID parameters of a hybrid single-area power systems. Later on, nature inspired evolutionary and soft computing schemes (like, the non-dominated sorting genetic algorithm-II, firefly algorithm, imperialist competitive algorithm) are introduced to design optimal FO-PID controllers for multi-area power systems [12–14]. In these intelligent optimization schemes, the multi-objective functions are framed using integral square indices such as *ITAE*, *ISE*, *ISDCO* (integral of the squared deviation in controller output) and other figure of merits to tune PID parameters. Although the aforementioned LFC schemes have shown their effectiveness and dominance over classical approach, there are deficiencies due to heavy computational burden, premature convergence during optimization process and sluggish disturbance

* Corresponding author.
E-mail address: sahajsaxena11@gmail.com.

https://doi.org/10.1016/j.ijepes.2018.07.005
Received 27 November 2017; Received in revised form 23 May 2018; Accepted 5 July 2018

attenuation.

IMC technique is a control strategy that has been successfully used for few decades [15–20]. It is observed that simplicity, robustness, sub-optimality and wide area applicability are some features that have popularized IMC among control scientists and practitioners. After the introduction of IMC scheme in FO systems and control for last 2–3 years, the FO-PID got a new way for its synthesis and tuning (See [21] and the references therein). Moreover, in literature on one hand, CRONE (abbreviation of "Commande Robuste d'Ordre Non Entier" which means "non integer order robust control") principle is highly popular for designing FO controller [22] and on the other hand IMC is famous control scheme for designing IO controller. Fortunately, the pioneer work of Maâmar & Rachid [23] bridges both control schemes to build FO controller. Through this method, the controller acquires the FO-PID form via IMC methodology and tuning scheme is evolved using CRONE principle.

Motivated by the celebrated work of [23], the FO controller design scheme is proposed in this paper which make use of reduced-order modeling to acquire the dominant features of the higher-order plant. Also to the best of author's knowledge, such LFC scheme is missing in power control research. Therefore in this paper, a FO-PID based on IMC and CRONE schemes is proposed for frequency regulation of single and multi-area power systems. The proposed design requires only frequency domain specifications particularly phase margin and gain crossover frequency as a prerequisite. The main advantages of this work is that: (i) the proposed scheme exhibits robustness as the controller parameters, tuned with the help of gain and phase margin specifications, works well when parametric uncertainties are present in power plant, (ii) the controller is optimal as it minimizes the integral error indices, and (iii) for executing LFC, substantial improvements are observed in the performance using the proposed method in comparison to the recently developed methods.

2. Description of LFC model

Electric power systems are complex non-linear dynamical systems consisting of numerous generators and loads. However for modeling purpose, all the generators are lumped into single equivalent generator and likewise for loads. Since, power systems are exposed to small load changes, the system can be adequately represented by its linear model [2,33]. The basic power system notations are presented in Table 1.

2.1. Single-area power system

The block diagram of a single-area power system supplying power to single service area through single generator is shown in Fig. 1. The dynamics of this plant which consists of governor, non-reheated turbine, and load and machine can be written as

$$\frac{\mathrm{d}}{\mathrm{d}t}\Delta f(t) = -\frac{1}{T_P}\Delta f(t) + \frac{K_P}{T_P}(\Delta P_G(t) - \Delta P_d(t)) \tag{1}$$

Table 1
Nomenclature of Basic Power Systems Terms.

$\Delta f(t)$	Incremental change in frequency (Hz)
$\Delta P_d(t)$	Load disturbance (p.u. MW)
$\Delta P_G(t)$	Incremental change in generator output (p.u. MW)
$\Delta X_G(t)$	Incremental change in governor valve position (p.u. MW)
K_P	Electric system gain
T_P	Load and machine time constant (s)
T_T	Non-reheated turbine time constant (s)
T_r	Reheated turbine time constant (s)
T_w	Hydro turbine time constant (s)
T_G	Governor time constant (s)
c	Percentage of the power generated in the reheat portion
R	Speed regulation due to governor action (Hz/p.u. MW)
B_i	Frequency bias (p.u. MW/Hz)

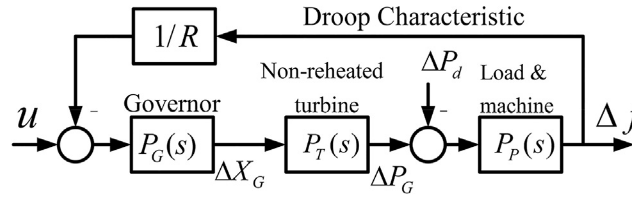

Fig. 1. Block diagram of single-area power system.

$$\frac{\mathrm{d}}{\mathrm{d}t}\Delta P_G(t) = -\frac{1}{T_T}\Delta P_G(t) + \frac{1}{T_T}\Delta X_G(t) \tag{2}$$

$$\frac{\mathrm{d}}{\mathrm{d}t}\Delta X_G(t) = -\frac{1}{RT_G}\Delta f(t) - \frac{1}{T_G}\Delta X_G(t) + \frac{1}{T_G}u(t) \tag{3}$$

In terms of transfer function model, the governor is

$$P_G(s) = \frac{1}{T_G s + 1}, \tag{4}$$

the non-reheated turbine is

$$P_T(s) = \frac{1}{T_T s + 1} \tag{5}$$

and the load and machine is

$$P_P(s) = \frac{K_P}{T_P s + 1} \tag{6}$$

Now using (4)–(6), the whole plant can be written as

$$\frac{\Delta f(s)}{u(s)} = P(s) = \frac{P_G(s)P_T(s)P_P(s)}{1 + P_G(s)P_T(s)P_P(s)/R} = \frac{K_P}{a_3 s^3 + a_2 s^2 + a_1 s + a_0} \tag{7}$$

where

$$a_3 = T_G T_T T_P,\quad a_2 = T_G T_T + T_P T_T + T_P T_G,$$
$$a_1 = T_G + T_T + T_P,\quad a_0 = 1 + \tfrac{K_P}{R} \tag{8}$$

As LFC is a disturbance rejection problem, so our aim is to find a control law: $u(s) = -C(s)\Delta f(s)$ such that $\lim_{t\to\infty}\Delta f(t) = 0$, for all ΔP_d.

Remark 1. Nonlinearities (backlash and wind-up problems) in the speed control are normally neglected except for rate limiter and the limits on valve position. All damping torque to prime-mover, generator and the HVDC system are also assumed to be negligible.

3. Design tools

In this section, we put forward few prerequisites to present our proposed work. Throughout the paper, the real and natural numbers are symbolized by $\mathbb{R}$ and $\mathbb{N}$, respectively. Further $\mathbb{R}^+$ denotes the real positive numbers. For any signal $x(t)$, its Laplace transform is denoted by $X(s)$. A stable continuous-time, linear time-invariant finite dimensional single-input single-output system described by a rational proper transfer function $G(s)$ is considered whose order is denoted with $\rho(G)$. A stable system $G(s)$ is a minimum-phase system if the zeros of the system are stable, *i.e.*, roots of the numerator polynomial are in left-half of complex s-plane.

3.1. Fractional-order system

Here, a brief exposition of FO operators and their properties are given. Fractional calculus is actually the generalization of IO integration and differentiation to any arbitrary real number. It is an old concept in mathematics however in control engineering it has witnessed a remarkable progress from last one decade after the introduction of FO controllers [8,9,24]. Now, we introduce the notion of generalized FO operators. The continuous integro-differential operator of order $\alpha \in \mathbb{R}$ (often denoted by ${}_x\mathrm{D}_t^{\alpha}$, where x and t denote the limits of the operation) is defined as

$$ {}_x\mathrm{D}_t^{\alpha} = \begin{cases} \mathrm{d}^{\alpha}/\mathrm{d}t^{\alpha} & \alpha > 0, \\ 1 & \alpha = 0, \\ \int_x^t (\mathrm{d}\tau)^{-\alpha} & \alpha < 0. \end{cases} $$

In this paper, we define the FO system using the differential equation of the form

$$ \sum_{i=1}^{m} a_i \mathrm{D}_t^{\mu_i} y(t) = \sum_{i=1}^{l} b_i \mathrm{D}_t^{\nu_i} u(t) $$

where $\mu_m > \mu_{m-1} > ... > \mu_1 > 0$ and $\nu_l > \nu_{l-1} > ... > \nu_1 > 0$ are strictly positive real numbers and $(a_i, b_i) \in \mathbb{R}^2$. On interpreting this equation in the popular Caputo sense (see Definition 1) and applying the Laplace transform for zero initial condition, the transfer function can be obtained as

$$ G(s) = \frac{\sum_{i=1}^{l} b_i s^{\nu_i}}{\sum_{i=1}^{m} a_i s^{\mu_i}} $$

where $a_m \neq 0$ and $\mu_m > \nu_l$ is assumed so that $G(s)$ is strictly proper.[1]

Definition 1. The Caputo definition of FO derivative of order α of a continuous function f: $\mathbb{R}^+ \to \mathbb{R}$ is defined as:

$$ {}_a\mathrm{D}_t^{\alpha} f(t) = \frac{1}{\Gamma(n-\alpha)} \int_a^t \frac{f^{(n)}(\tau)}{(t-\tau)^{\alpha-n+1}} d\tau, \quad \forall\, n-1 < \alpha < n $$

where $f^{(n)}(t)$ is the n^{th} derivative of $f(t)$ with respect to t, $n \in \mathbb{N}$ and $\Gamma(\bullet)$ is Gamma function.[2] The Laplace transform of this derivative is given by

$$ \int_0^t e^{-st}\, {}_a\mathrm{D}_t^{\alpha} f(t) \mathrm{d}t = s^{\alpha} F(s) - \sum_{k=0}^{n} s^{\alpha-k-1} f^{(k)}(0) $$

Remark 2. When $\alpha = n \in \mathbb{N}$ then ${}_a\mathrm{D}_t^{\alpha} f(t) = \frac{\mathrm{d}^n}{\mathrm{d}t^n} f(t)$.

Remark 3. In literature, various definitions of fractional calculus are presented but Caputo definition is highly popular particularly in engineering. In Caputo definition, the initial conditions are of integer-order (*i.e.*, derivative of constant is zero) which make them easier to interpret because the IO derivatives of involved variables have well-established physical meanings and can be easily obtained by experimental means.

Like the IO system where the building blocks of system are integrators and differentiators, the FO system also constitutes FO integrators and differentiators as their basic elements.

Definition 2. The transfer function of FO integrator is defined as

$$ G(s) = \frac{1}{s^p}, \quad p \in (0, 1). \tag{9} $$

For $p = 1$, $G(s)$ is a simple pure integrator. As p tends towards 0, the effect of integration operation eliminates because $s^0 = 1$.

Remark 4. In control theory, the addition of pure integrator retards the speed of response but here the FO integrator relaxes this constraint.

Putting $s = \mathrm{j}\omega$ in (9), the spectral transfer function is obtained as

$$ G(\mathrm{j}\omega) = \frac{1}{\omega^p \left[\cos(\frac{p\pi}{2}) + \mathrm{j}\sin(\frac{p\pi}{2})\right]} $$

[1] A strictly proper transfer function satisfies $G(s) \to 0$ as $s \to \infty$.

[2] The Gamma function is defined by $\Gamma(p) = \int_0^{\infty} t^{p-1} e^{-t} \mathrm{d}t$, $\Re(p) > 0$

whose magnitude $A(\omega) = \frac{1}{\omega^p}$ in dB is given by

$$ M(\omega) = -20p\log(\omega) \tag{10} $$

and the phase is

$$ \phi(\omega) = \arg\left[\frac{1}{\omega^p} \mathrm{j}^{-p}\right] = -\frac{p\pi}{2} \tag{11} $$

From (10) and (11), it is clear that the magnitude of a FO integrator in the frequency domain drops at a rate of $20p$ dB/dec and its phase is $-p\pi/2$ throughout the domain. Whereas the IO integrator yields fixed drop at a rate of -20 dB/dec in magnitude and $-\pi/2$ in phase response. This may hinders the stability and robustness of the closed-loop system. Thus the FO integrator introduces new degrees of flexibility that simplifies the design of high performance controller.

3.2. IMC technique [15,16]

IMC is a model predictive based control technique which utilizes an additional plant model to predict the output and rectify the error between desired and actual output. Fig. 2 shows the structure of the IMC controller in which $P(s)$ is a plant and its model is $\widetilde{P}(s)$. The IMC controller $Q(s)$ is composed of inverse of $\widetilde{P}(s)$ cascaded with IMC filter $F(s)$. The output of the plant is y_o for input y_i and disturbance is d. The output is formulated as

$$ Y_o(s) = \frac{\widetilde{P}^{-1}(s)P(s)F(s)}{1 + F(s)\widetilde{P}^{-1}(s)\Delta P(s)} Y_i(s) + \frac{1 - F(s)\widetilde{P}^{-1}(s)P(s)}{1 + F(s)\widetilde{P}^{-1}(s)\Delta P(s)} D(s) \tag{12} $$

where $\Delta P(s) = P(s) - \widetilde{P}(s)$ is the plant-model mismatch. If the model of plant is an exact representation of the real plant, *i.e.*, $\widetilde{P}(s) = P(s)$, and $F(s) = 1$ then from (12) we get $Y_o(s) = Y_i(s)$ for all $D(s)$. Thus, perfect tracking and disturbance rejection can be achieved in this ideal case. However, such control strategy cannot be directly implemented in the case where the model of the plant is strictly proper or non-minimum phase.

Generally in real time scenario, plant-model mismatching is present and the uncertainty in the plant increases with frequency. At this stage, robustness against plant-model mismatch can be improved by means of filter $F(s)$. This filter is designed to add poles to $\widetilde{P}(s)$ and is chosen such that the closed-loop system retains its asymptotic tracking properties (*i.e.*, zero offset at steady state for asymptotically constant inputs and step type disturbances). It is usually a low-pass filter of the type

$$ F(s) = \frac{1}{(1 + \lambda s)^n} \tag{13} $$

where λ is the filter parameter that fixes the bandwidth of the closed-loop system and $\rho(F) = n$ is chosen according to the order of $\widetilde{P}(s)$. Using this approach, $Q(s)$ parameters are linked in a unique straightforward manner to $\widetilde{P}(s)$ parameters. In (13), λ is now the only parameter to be tuned to influence the speed of response of the closed-loop system. This λ is also detuned to maintain the robustness in presence of plant-model uncertainties. Therefore a trade-off is imposed for sacrificing performance to attain robustness which is inherent to any control system.

The IMC structure is complex for practical implementation, and it is usually rearranged into its equivalent conventional feedback control structure as shown in Fig. 3. The relation between $Q(s)$ and $\widetilde{P}(s)$ of Fig. 2 and $C(s)$ of Fig. 3 is given by

$$ C(s) = \frac{Q(s)}{1 - Q(s)\widetilde{P}(s)} \tag{14} $$

Remark 5. The main advantage of the IMC technique is the stability of the closed-loop system. As the IMC structure is internally stable (*i.e.*, $P(s)$ and $Q(s)$ are stable), therefore its equivalent conventional feedback control structure is also stable.

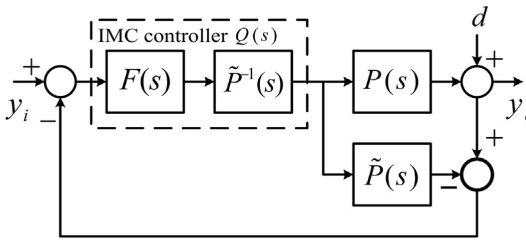

Fig. 2. Schematic diagram of the IMC.

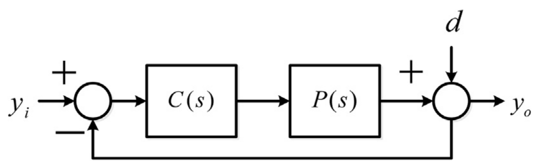

Fig. 3. Schematic diagram of the conventional feedback control structure.

Remark 6. At many instances, the actual plant exhibits non-minimum phase characteristics (RHP zeros or delay). In such cases, IMC procedure is applied by segregating the plant into its minimum phase and non-minimum phase elements, i.e.,

$$\bar{P}(s) = \bar{P}_-(s)\bar{P}_+(s)$$

where $\bar{P}_-(s)$ is minimum phase part and $\bar{P}_+(s)$ is non-minimum phase part. And the minimum phase element is used to design the controller.

3.3. Reduced-order modeling

Reduced-order modeling is a tool which simplifies the high-order complex real plant into its adequate low-order model such that the important features of the original system are retained in the reduced model. This tool reduces the computational effort for analyzing the complex dynamics of the real plant by removing any redundant information. Thus, it helps in designing and developing the controller with less effort and at cheaper cost [25–28]. In control system, it pursues the following definition.

Definition 3. Let $B(s)$: $u \mapsto y$ be the original system with $\rho(B) = v$, then the reduced-order modeling is a technique to find a reduced-order model $\widetilde{B}(s)$: $u \mapsto \widetilde{y}$ with $\rho(\widetilde{B}) = w$ so that $w < v$ and for the same input $u(t) \in L_2$, $\widetilde{y}(t) \approx y(t)$.

The reduced-order modeling scheme must satisfies the following properties: (i) it targets to minimize the infinity norm approximation error defined by $E(s) = \| B(s) - \widetilde{B}(s) \|_\infty = \sup_{\omega \geqslant 0} |B(\omega) - \widetilde{B}(\omega)|$, for all $\omega \in \mathbb{R}$; (ii) system properties, such as stability, are preserved; and (iii) the procedure is computationally efficient. In this paper, we follow the Routh approximation based reduced-order modeling method [29]. In this method, the *Routh table* for the original plant is developed, and then the reduced model is constructed in such a way that the coefficients of its Routh table matches up to a given order with that of the original plant. The detailed procedure is provided in the later section.

3.4. CRONE principle

The CRONE principle relies on the concept of robustness in order to maintain time and frequency domain performance measures (iso-damping property, stability margin) using complex fractional integration [30,31]. It actually includes the concept of Bode's ideal transfer function. In CRONE principle, the open-loop transfer function $L(s)$ is the transfer function of a FO integrator as $L(s) = \frac{1}{\tau s^\gamma}$, $\gamma \in (1, 2)$ and $\tau > 0$, where

$$\omega_{gc} = \tau^{-1/\gamma} \tag{15}$$

is a gain crossover frequency.[3] Thus in open-loop, it has constant slope of -20γ dB/s and phase curve is horizontal line at $-\frac{\gamma\pi}{2}$. The Nyquist curve is a straight line through the origin with argument $-\frac{\gamma\pi}{2}$. Let us now consider a unity feedback system with $P_o(s) := P(s)C(s) = L(s)$ inserted in the forward path as shown in Fig. 3 for which the closed-loop transfer function can be written as

$$T(s) := \frac{P_o(s)}{1 + P_o(s)} = \frac{1}{1 + \tau s^\gamma} \tag{16}$$

Substituting $s = \mathrm{j}\omega$ and $\mathrm{j} = e^{\mathrm{j}\frac{\pi}{2}}$, the spectral transfer function of $T(s)$ is

$$T(\mathrm{j}\omega) = \frac{1}{\left(1 + \tau\omega^\gamma \cos\frac{\gamma\pi}{2}\right) + \mathrm{j}\tau\omega^\gamma \sin\frac{\gamma\pi}{2}} \tag{17}$$

The amplitude and phase of $T(\mathrm{j}\omega)$ can be evaluated as

$$|T(\mathrm{j}\omega)|_{\mathrm{dB}} = 20\log\frac{1}{\sqrt{1 + 2\tau\omega^\gamma \cos\frac{\gamma\pi}{2} + (\tau\omega^\gamma)^2}} \tag{18}$$

and

$$\arg[T(\mathrm{j}\omega)] = -\arctan\left[\frac{\tau\omega^\gamma \sin\frac{\gamma\pi}{2}}{1 + \tau\omega^\gamma \cos\frac{\gamma\pi}{2}}\right] \tag{19}$$

From (18) and (19), it is obvious that at $\omega = 0$, $T(\mathrm{j}\omega) = 0$ and $\arg[T(\mathrm{j}\omega)] = 0$. The asymptotic behavior of $T(\mathrm{j}\omega)$ at $\omega \to \infty$ is $T(\mathrm{j}\omega) \approx -20\gamma\log(\tau\omega)$ and $\arg[T(\mathrm{j}\omega)] \approx -\frac{\gamma\pi}{2}$. See appendix A for evaluation. Hence, the frequency response resembles with the low-pass filter.

Definition 4. The frequency at which the maximum value of the spectral transfer function (known as resonance peak M_r) is attained is called resonance frequency ω_r.

The resonance peak M_r at resonance frequency ω_r is given by the formula

$$M_r = \frac{1}{\sin\frac{\gamma\pi}{2}}, \quad \omega_r = \frac{1}{\tau}\left|\cos\frac{\gamma\pi}{2}\right|^{\frac{1}{\tau}}$$

Refer appendix B for proof. The natural frequency and damping ratio are given by

$$\omega_p = \frac{1}{\tau}\sin\pi\left(1 - \frac{1}{\gamma}\right)$$

and

$$\zeta = -\cos\frac{\pi}{\gamma}$$

respectively. See appendix C for derivation. Also, the phase margin[4] is

$$\phi = \pi\left(1 - \frac{\gamma}{2}\right) \tag{20}$$

Now it is clear that when the system parameter τ varies while keeping the γ fixed, only the rise time (*i.e.*, natural frequency) and speed of the response (*i.e.*, resonance frequency) varies while ensuring the constant resonance peak and phase margin and thus correspondingly a constant damping ratio and overshoot in time domain. Therefore, we can shape the output response close to the desired response by varying the reference tuning parameters (γ, ω_{gc}).

[3] A gain crossover frequency, $\omega_{gc} \in [0, \infty)$, for $L(s)$, is a frequency at which $|L(\mathrm{j}\omega_{gc})| = 1$.

[4] The phase margin for $T(s)$ is defined by $\phi = \arg[L(\mathrm{j}\omega_{gc})] + \pi$.

4. Proposed FO-PID controller design scheme

We now present our proposed controller design scheme.

4.1. Controller framework

Let us consider an all-pole plant to be controlled as

$$P(s) = \frac{K}{D(s)},\ \ K > 0$$

where $D(s) = d_n s^n + d_{n-1}s^{n-1} + \ldots + d_1 s + d_0$, and $\{d_i\}_{i=1,2,\ldots,n} \in \mathbb{R}$ such that $P(s)$ is stable. The general form of second-order reduced-model can be written as

$$\widetilde{P}(s) = \frac{k}{\widetilde{d}_2 s^2 + \widetilde{d}_1 s + \widetilde{d}_0},\ \ k > 0 \tag{21}$$

where $\{\widetilde{d}_i\}_{i=1,2,3} \in \mathbb{R}^+$. To design IMC based controller, a FO filter of form

$$\widetilde{F}(s) = \frac{1}{1 + \lambda s^{\psi+1}},\ \ 0 < \psi < 1;\ \lambda \geqslant 0 \tag{22}$$

is chosen in place of filter of form (13). The IMC controller is determined as

$$Q(s) = \frac{\widetilde{d}_2 s^2 + \widetilde{d}_1 s + \widetilde{d}_0}{k(1 + \lambda s^{\psi+1})}.$$

Using (14), the equivalent conventional feedback controller is

$$C(s) = \frac{1}{s^{\psi}}\frac{\widetilde{d}_2 s^2 + \widetilde{d}_1 s + \widetilde{d}_0}{k\lambda s}$$

which can be further rearranged as

$$C(s) = k_c\left(1 + \frac{1}{\tau_i s} + \tau_d s\right)\left(\frac{1}{s^{\psi}}\right) \tag{23}$$

where $k_c = \widetilde{d}_1/(k\lambda)$, $\tau_i = \widetilde{d}_1/\widetilde{d}_0$, $\tau_d = \widetilde{d}_2/\widetilde{d}_1$.

Remark 7. Eq. (23) represents $C(s)$ as a FO-PID controller which is a combination of conventional IO type PID controller and FO integrator $1/s^{\psi}$.

4.2. Tuning of controller

In the proposed controller, only two parameters (λ, ψ) are unknown. To determine these tuning parameters, we present few immediate results derived from discussions in Section 3.

Lemma 1. *A good IMC based control is obtained if the reduced-order model $\widetilde{P}(j\omega)$ approximates the magnitude of real plant $P(j\omega)$ within achievable bandwidth.*

Proof. From (12), we can say that a good control (*i.e.*, $Y_o(s) \approx Y_i(s)$ for all $D(s)$) is obtained when

$$|\widetilde{P}^{-1}(j\omega)\Delta P(j\omega)| \approx 0 \tag{24}$$

and

$$|\widetilde{P}^{-1}(j\omega)P(j\omega)| \approx 1 \tag{25}$$

within achievable bandwidth. Therefore, (24) and (25) imply that

$$|\widetilde{P}(j\omega)| \approx |P(j\omega)| \tag{26}$$

Theorem 1. *For a minimum-phase system, the closed-loop transfer function derived using IMC technique is exactly or approximately the transfer function of the IMC filter used.*

Proof. Consider a minimum-phase plant $G(s)$ and its approximated model as $\widetilde{G}(s)$. The IMC controller with filter $F(s)$ can be obtained as $Q(s) = \widetilde{G}^{-1}(s)F(s)$. The corresponding conventional feedback controller is

$$C(s) = \frac{\widetilde{G}^{-1}(s)F(s)}{1-F(s)}$$

The closed-loop transfer function $T(s) := \frac{C(s)G(s)}{1 + C(s)G(s)}$, now becomes

$$T(s) = \frac{G(s)\widetilde{G}^{-1}(s)F(s)}{1 + (G(s)\widetilde{G}^{-1}(s)-1)F(s)} \tag{27}$$

To evaluate $T(s)$, two cases are considered.

Case 1: When $\widetilde{G}(s) = G(s)$, *i.e.*, the case of perfect control, then from (27) we have

$$T(s) = F(s) \tag{28}$$

Case 2: When $\widetilde{G}(s) \approx G(s)$, *i.e.*, the case of good control (Lemma 1), then from (27) we get

$$T(s) \approx F(s) \tag{29}$$

Eqs. (28) and (29) imply that the closed-loop transfer function of the system to be controlled using IMC technique is exactly or approximately the transfer function of the filter used. □

If $\widetilde{F}(s)$ described in (22) is used to design IMC controller, then from Theorem 1, we get $T(s) = \widetilde{F}(s)$. Now, this FO filter can be treated as a reference closed-loop model as per the CRONE principle. On comparing (22) and (16), we get $\tau = \lambda$ and $\gamma = \psi + 1$ and substituting these values in (15) and (20), we get

$$\psi = \frac{\pi-\phi_m}{\pi/2}-1;\ \lambda = 1/\omega_{gc}^{\psi+1} \tag{30}$$

Thus, with the help of desired ϕ_m and ω_{gc} the proposed controller can be tuned.

Remark 8. In general practice, the bandwidth of the overall control system is considered greater than that of the plant whereas it is opposite in the case where plant has non-minimum phase characteristics or input constraints.

4.3. Rejection capacity and stability of control system

.

Corollary 1. Under the assumption that there is almost zero plant model mismatching, the disturbance response for step type input is zero when FO filter of form (22) is used.

Proof. The immediate result of Theorem 1 gives $T(s) = F(s)$. The transfer function from disturbance to output is the sensitivity function $S(s)$ and is given by

$$\frac{Y(s)}{D(s)} = S(s) := 1-T(s) = \frac{\lambda s^{\psi+1}}{1 + \lambda s^{\psi+1}}$$

Therefore, for a unit step input $D(s) = \frac{1}{s}$, the output $Y(s)$ is

$$Y(s) = \frac{1}{s}\frac{\lambda s^{\psi+1}}{1 + \lambda s^{\psi+1}}$$

On applying *final value theorem* of signal processing theory, we get

$$\lim_{t\to\infty} y(t) = \lim_{s\to 0} sY(s) = 0$$

□

Thus it is clear that the proposed controller has capability to reject the disturbance. Now we examine the stability of the closed-loop system. The stability analysis methodology for FO system is different from that of the IO system. Here, the stability is defined using extended Matignon's Theorem as stated below.

Theorem 2. *If p_i's are the roots of a characteristic equation $\Delta(s) = 1 + \sum_{i=1}^{m} a_i s^{\mu i}$, then the system is bounded-input, bounded-output* *stable if and only if*

$$|\arg(p_i)| > \frac{\mu\pi}{2} \tag{31}$$

provided

$$0 < \mu < 2 \tag{32}$$

Proof. The proof could be performed in a way as given in [32].

From Theorem 1, the denominator of $F(s)$ in (22) acts as a characteristic equation:

$$\Delta(s) = 1 + \lambda s^{\frac{y}{x}} \tag{33}$$

where $\frac{y}{x} = 1 + \psi$; $x, y \in \mathbb{N}$ and $1 < \frac{y}{x} < 2$. Let $\sigma = s^{\frac{1}{x}}$ then (33) becomes $\Delta(\sigma) = 1 + \tau s^y$ whose roots are

$$\{p_l\}_{l=0,1,\ldots,(y-1)} = \left|\frac{1}{\tau}\right| e^{j\frac{1+2l}{y}\pi} \tag{34}$$

According to Theorem 2, for stability of (33), it is required to prove that $|\arg(p_i) = \frac{1}{\tau}e^{j\frac{1+2l}{y}\pi}| > \frac{\pi}{2x}$. From (32), it can be said that $0 < \mu < 2$ or $0 < \frac{1}{x} < 2$. Since $\frac{y}{x} < 2$ or $y < 2x \Rightarrow \frac{1}{y} > \frac{1}{2x}$. Therefore, it is evident that $\frac{(1+2l)\pi}{y} > \frac{\pi}{2x}$. Thus, the closed-loop FO system is stable.

5. FO-PID controller design for LFC

We now apply the proposed scheme to solve LFC problem.

5.1. Two-area power system

The LFC design can be extended to multi-area interconnected power systems. Without the loss of generality, the LFC problem for a two-area power system is presented in this paper. Fig. 4(a) depicts the simplified diagram of this two-area system and schematic diagram of i^{th}-area is shown in Fig. 4(b) [34]. In multi-area system, not only the frequency deviation but also the tie-line power must return to its scheduled value during load fluctuations in any area. Therefore, a composite measure,

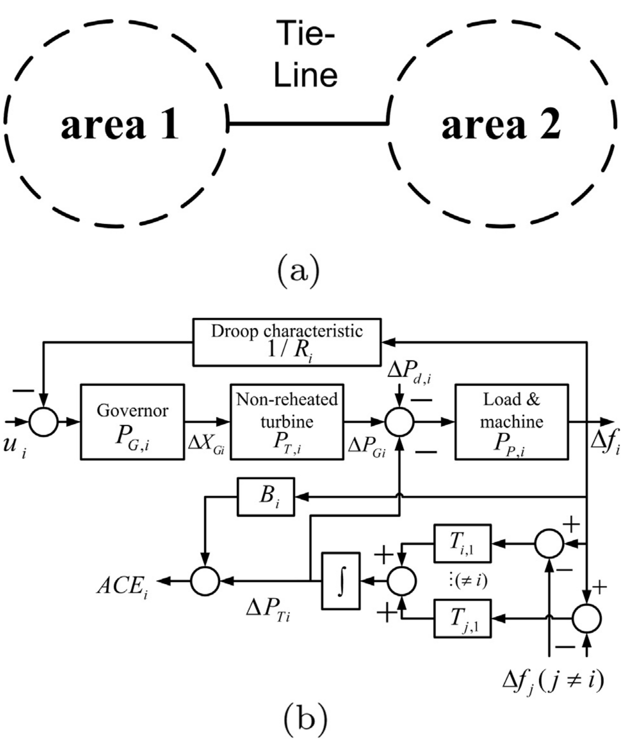

Fig. 4. (a) Block diagram of two-area power system and (b) the functional block diagram of i^{th} control area in LFC framework.

called area control error (ACE) is utilized in controller as a feedback variable. For two-area system, ACE_i, $i = 1, 2$ are defined as

$$ACE_1(s) = \Delta P_T(s) + B_1\Delta f_1(s)$$

$$ACE_2(s) = -\Delta P_T(s) + B_2\Delta f_2(s)$$

where $\Delta P_T = \frac{T_{12}}{s}(\Delta f_1 - \Delta f_2)$ is the tie-line power deviation (p.u.MW) from the scheduled tie-line exchange power, and T_{12} is tie-line synchronizing coefficient (p.u.MW/radian) between area 1 and 2. For two-area power system, decentralized controllers $C_1(s)$ and $C_2(s)$ can be synthesized assuming $\Delta P_T(s) = 0$ which implies $T_{12} = 0$. In this case, the transfer function of i^{th} control area is given by

$$P_i(s) = B_i\frac{P_{G,i}(s)P_{T,i}(s)P_{P,i}(s)}{1 + P_{G,i}(s)P_{T,i}(s)P_{P,i}(s)/R_i} \tag{35}$$

where $P_{G,i}(s)$, $P_{T,i}(s)$, $P_{P,i}(s)$ are the transfer functions of governor, the turbine and the generator for i^{th} area. Lastly, our aim is to develop decentralized regulation law which takes the form: $u_i(s) = -C_i(s)ACE_i(s)$ so that $\lim_{t\to\infty} ACE_i(t) = 0$, for all $\Delta P_{d,i}$.

5.2. Reduced model identification

Power systems are highly large interconnected network of power apparatus. Even a single-area power system plant transfer function (7) containing single generator is of third-order. Therefore for fast and cost efficient planning, operations and control, reduced-order models of power systems are necessary. Here, Routh approximation model reduction scheme [29] is applied to obtain second-order model of power system.

For a single-area plant (7), let the reduced model is $\widetilde{P}(s)$ with $\rho(\widetilde{P}) = 2$. To apply Routh approximation method [29], we first reciprocate $P(s)$ using relation

$$\hat{P}(s) = \frac{1}{s}P\left(\frac{1}{s}\right) \tag{36}$$

which gives

$$\hat{P}(s) = \frac{K_P s^2}{a_0 s^3 + a_1 s^2 + a_2 s + a_3} \tag{37}$$

Now, expand $\hat{P}(s)$ in the following canonical form:

$$\hat{P}(s) = \beta_1 E_1(s) + \beta_2 E_1(s)E_2(s) + \beta_3 E_1(s)E_2(s)E_3(s) \tag{38}$$

where $\{\beta_i\}_{i=1,2,3}$ are constants, $E_1(s) = 1 + \alpha_1 s$, $E_2(s)$ and $E_3(s)$ are functions of α_2 and α_3. Since we are interested in calculating the reduced model, therefore as described in [29] the second-order reduced model is given by

$$\hat{\widetilde{P}}(s) = \frac{\alpha_2\beta_1 s + \beta_2}{\alpha_2\alpha_1 s^2 + \alpha_2 s + 1} \tag{39}$$

where $\alpha_{1,2}$ can be calculated with the help of α-table as shown in Table 2 and $\beta_{1,2}$ are given by $\beta_1 = K_P/a_1$ and $\beta_2 = 0$. On substituting the values of $\alpha_{1,2}$ and $\beta_{1,2}$ in (39) and further using relation (36), we get the reduced model $\widetilde{P}(s)$ as:

$$\widetilde{P}(s) = \frac{a_1 K_P}{(a_1 a_2 - a_0 a_3)s^2 + a_1^2 s + a_0 a_1} \tag{40}$$

Table 2
α–table.

	a_0	a_2
$\alpha_1 = \frac{a_0}{a_1}$	a_1	a_3
$\alpha_2 = \frac{a_1^2}{a_1 a_2 - a_0 a_3}$	$\frac{a_1 a_2 - a_0 a_3}{a_1}$	

Remark 9. In case of multi-area power system, we know that only B_i is an additional variable which is to be multiplied with each control area plant model (refer (35)). Therefore, same reduced model multiplied by B_i is obtained for each control area.

5.3. Controller synthesis

For single-area power system, the model in (40) resembles with (21), therefore one can write

$$k = a_1 K_P,\ \tilde{d}_2 = a_1 a_2 - a_0 a_3,\ \tilde{d}_1 = a_1^2,\ \tilde{d}_0 = a_0 a_1 \tag{41}$$

On substituting these values of (41) in (23), the proposed FO-PID controller can be obtained as

$$C(s) = \frac{a_1}{\lambda K_P}\left(1 + \left(\frac{a_0}{a_1}\right)\frac{1}{s} + \left(\frac{a_1 a_2 - a_0 a_3}{a_1^2}\right)s\right)\left(\frac{1}{s^{\psi}}\right) \tag{42}$$

The same procedure is applied for multi-area power system. Therefore, without the loss of generality, for i^{th} control area, the decentralized controller $C_i(s)$ is given by

$$C_i(s) = \frac{a_{1,i}}{\lambda B_i K_{P,i}}\left(1 + \left(\frac{a_{0,i}}{a_{1,i}}\right)\frac{1}{s} + \left(\frac{a_{1,i} a_{2,i} - a_{0,i} a_{3,i}}{a_{1,i}^2}\right)s\right)\left(\frac{1}{s^{\psi_i}}\right) \tag{43}$$

6. Simulation tests

For executing the proposed scheme for single and two-area configuration, simulations are carried out using Intel® CORE™ i7 processor through MATLAB® and Simulink® (using FOMCON toolbox available athttp://fomcon.net/fomcon-toolbox/download/). The fractional derivative has been implemented by the Oustaloup recursive filter approximation choosing a frequency range of $[10^{-3}, 10^{3}]$ rad/s and order of filter $N = 5$. See appendix D for more information. The nominal parameters of power system plant are taken as [35]:

$$K_P = 120,\ T_P = 20,\ T_T = 0.3,\ T_G = 0.08,\ R = 2.4 \tag{44}$$

6.1. LFC design for single-area system

On substituting values of (44) in (8), the original plant in (7) is given by

$$P(s) = \frac{250}{s^3 + 15.88s^2 + 42.46s + 106.2} \tag{45}$$

and its reduced-model from (40) becomes

$$\tilde{P}(s) = \frac{18.38}{s^2 + 3.173s + 7.94} \tag{46}$$

The time and frequency domain responses of the original plant and the reduced model as shown in Fig. 5 confirms the resemblance of reduced model with the original one.

In order to achieve good disturbance rejection performance, the bandwidth of closed-loop control system should be considerably larger than the plant to be controlled. Keeping this fact in mind, we select $\omega_{gc} = 15$ rad/s for the closed-loop control system whereas for plant in closed-loop configuration without controller, $\omega_{gc} = 6.52$ rad/s. Further, $\phi_m = \pi/3$ is generally selected as a standard phase margin for tuning the controller. Now on applying the proposed method, the FO-PID controller is obtained as

$$C(s) = 6.2926\left(1 + \frac{2.5026}{s} + 0.3146s\right)\left(\frac{1}{s^{0.333}}\right) \tag{47}$$

To show the performance of the proposed controller, a step load $\Delta P_D = 0.01$ p.u. is applied at $t = 1$ s, and ± 50% uncertainty is also added in all the parameters of the power plants to observe the robustness of the controller, *i.e.*,

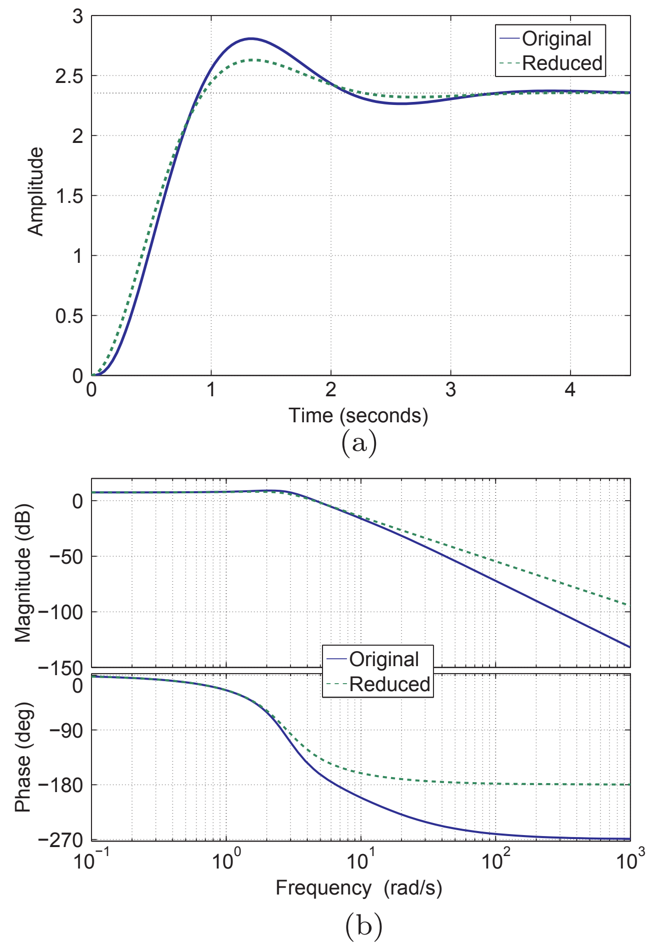

Fig. 5. (a) Step and (b) frequency responses of original and reduced-order model.

$$K_P = [60, 170],\ T_P = [10, 40],\ T_G = [0.04, 0.1],\ R = [1.2, 3.6] \tag{48}$$

Using this controller, disturbance rejection performance is obtained for nominal plant and perturbed plants (lower and upper bounds). The main advantage of the proposed controller is that the controller parameters need not to be changed even though there exist variations in the system parameters. To examine the efficiency of the proposed scheme, the frequency deviation responses of the power system using the proposed scheme is compared with the schemes recently developed by Tan [35], and Anwar and Pan [36] as shown in Fig. 6. It is observed that the proposed controller nullifies the change in frequency rapidly with least variations in its magnitude when compared with the LFC schemes designed by Tan [35] and Anwar and Pan [36]. Thus it can be claimed that proposed scheme gives better disturbance rejection performance with least settling time and overshoot for nominal as well as upper and lower bounds of perturbed system.

To measure the optimality of the proposed scheme, various performance measures defined in the form of integral error criterion ($ISE = \int_0^\infty \Delta f(t)^2 dt$; $IAE = \int_0^\infty |\Delta f(t)|\, dt$; $ITAE = \int_0^\infty t\, |\Delta f(t)|\, dt$; $IE) = \int_0^\infty \Delta f(t) dt$ are calculated in Table 3. Indirectly, these performance measures denote several characteristics like settling time, overshoot, speed of response, disturbance rejection, etc. They can be treated as objective function to investigate optimality of the controller. From Table 3, it is clear that the values of these objective functions are least for the proposed scheme in comparison to other schemes. Thus, the LFC system using proposed scheme is optimal in nature.

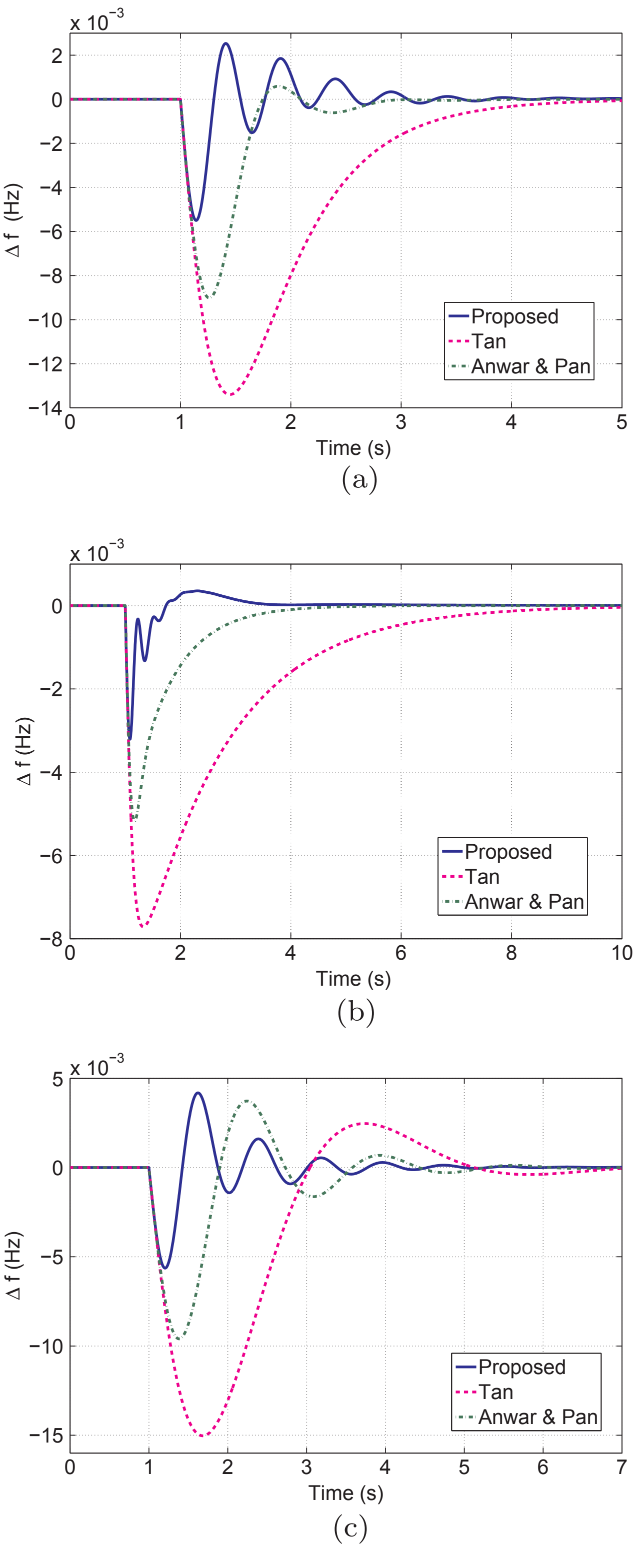

Fig. 6. Frequency deviation for (a) nominal, (b) lower and (c) upper models. The PID parameters of Tan [35] are: $k_c = 0.4036$, $k_i = 0.6356$, $k_d = 0.1832$ and Anwar & Pan [36] are: $k_c = 1.52$, $k_i = 2.50$, $k_d = 0.27$.

6.2. LFC design for two-area system

We extend our proposed scheme to design decentralized PID tuning for interconnected two-area power system. As mentioned in (35), one just needs to multiply the plant model by B_i to design a controller. For simplicity, the two areas are assumed to be identical and the nominal parameters of each area are same as given in (44). Therefore, the open-loop plant model ($P_1(s)$ and $P_2(s)$) of both the areas are represented by (45) which require $B_{1,2}$ as a multiplier. For LFC design, $B_1 = B_2 = 0.425$, $T_{12} = 0.3770$ and $T_{21} = 0.4398$ are taken. With the same controller tuning settings as given in single-area LFC design, we keep $\omega_{gc} = 15$ rad/s and $\phi_m = \pi/3$. Using these controller setting values and (43), the proposed decentralized controller $C_i(s)$, $i = 1, 2$ for each control area is obtained as

$$C_i(s) = 14.8061\left(1 + \frac{2.5026}{s} + 0.3146s\right)\left(\frac{1}{s^{0.333}}\right) \tag{49}$$

To investigate the efficiency and robustness of the controller, the parameters of area 2 are perturbed from their nominal values. From (48), the perturbed values (lower bound) are taken as

$$K_{P,2} = 60,\ T_{P,2} = 10,\ T_{T,2} = 0.15,\ T_{G,2} = 0.04,\ R_2 = 1.2.$$

The analysis is carried out by keeping the parameters of the area 1 in nominal state. Now, the step loads of $\Delta P_{d,1}(s) = 0.01$ at $t = 1$ s and $\Delta P_{d,2}(s) = 0.01$ at $t = 10$ s are applied to area 1 and area 2, respectively. The frequency and tie-line power deviations of the system using proposed controller, Tan [37], and Padhan and Majhi [38] schemes are shown in Figs. 7 and 8, respectively. It is observed that the frequency deviations in both areas settle to zero in minimum time with least overshoot by the proposed controller in comparison to the responses obtained by Tan, and Padhan and Majhi techniques. The similar improved performance in comparison to other approaches is also obtained in case of tie-line power as depicted in Fig. 8. Thus, the proposed controller rejects the load fluctuations and tolerate the uncertainties of the plant parameters efficiently.

6.3. LFC design for two-area system having reheated and hydro turbines

To extend the applicability of the proposed control scheme in LFC, we considered the two-area system in which the area 1 consists of a reheated turbine of the form

$$P_T(s) = \frac{cT_r s + 1}{(T_r s + 1)(T_T s + 1)} \tag{50}$$

and area 2 consists of hydro turbine of the form

$$P_T(s) = \frac{1 - T_w s}{1 + 0.5T_w s} \tag{51}$$

Remark 10. Eq. (51) denotes the non-minimum phase characteristics due to presence of RHP zero.

For area 1, the model parameters are taken as

$$K_P = 120,\ T_P = 20,\ T_T = 0.3,\ T_G = 0.08,\ R = 2.4,\ T_r = 4.2,\ c = 0.35 \tag{52}$$

The plant model now becomes

$$P(s) = \frac{87.5s + 59.52}{s^4 + 16.12s^3 46.24s^2 + 48.65s + 25.3} \tag{53}$$

On applying the Routh approximation based reduced-order modeling method [29], we get

$$\overline{P}(s) = \frac{1.572}{s^2 + 1.285s + 0.6683} \tag{54}$$

With the specifications $\omega_{gc} = 5$ rad/s and $\phi_m = \pi/3$, the proposed scheme using (43) yields

$$C_1(s) = 12.7923\left(1.285 + \frac{0.6683}{s} + s\right)\left(\frac{1}{s^{0.333}}\right) \tag{55}$$

For area 2, the hydro turbine power system with following parameters are considered:

$$K_P = 1,\ T_P = 6,\ T_w = 4,\ T_G = 0.2. \tag{56}$$

Table 3
Performance ($\times 10^{-5}$).

	Nominal				Lower				Upper			
Method	ISE	IAE	ITAE	IE	ISE	IAE	ITAE	IE	ISE	IAE	ITAE	IE
Proposed	**61.6**	**249.4**	**446.8**	**22.6**	**13.3**	**118**	**243.8**	**23**	**1.2**	**406**	**786**	**23**
Tan [35]	1355	981.8	1663	981.8	677.8	1524	4106	1524	21.1	2146	4842	1529
Anwar & Pan [36]	261.6	426.1	609.6	400	109.5	400	703.8	400	4.7	876	1756	400

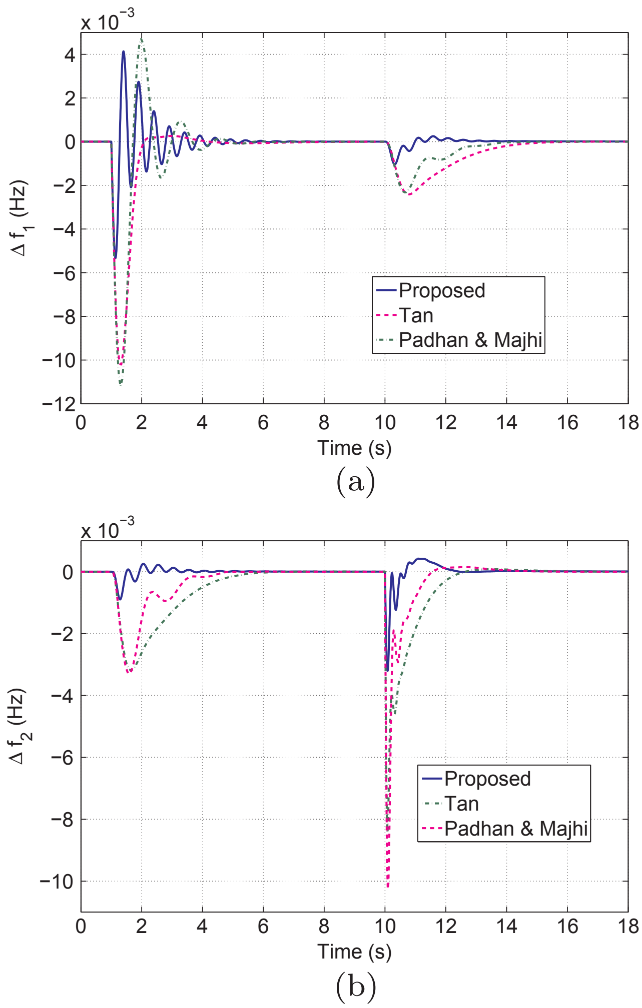

Fig. 7. Frequency deviation for (a) area 1 and (b) area 2. The parameters of PID from Tan [37] are: $k_c = 1.5692$, $k_i = 2.3966$, $k_d = 0.5259$, and Padhan & Majhi [38] are: $k_c = 1.9822$, $k_i = 0.5242$, $k_d = 0.1756$.

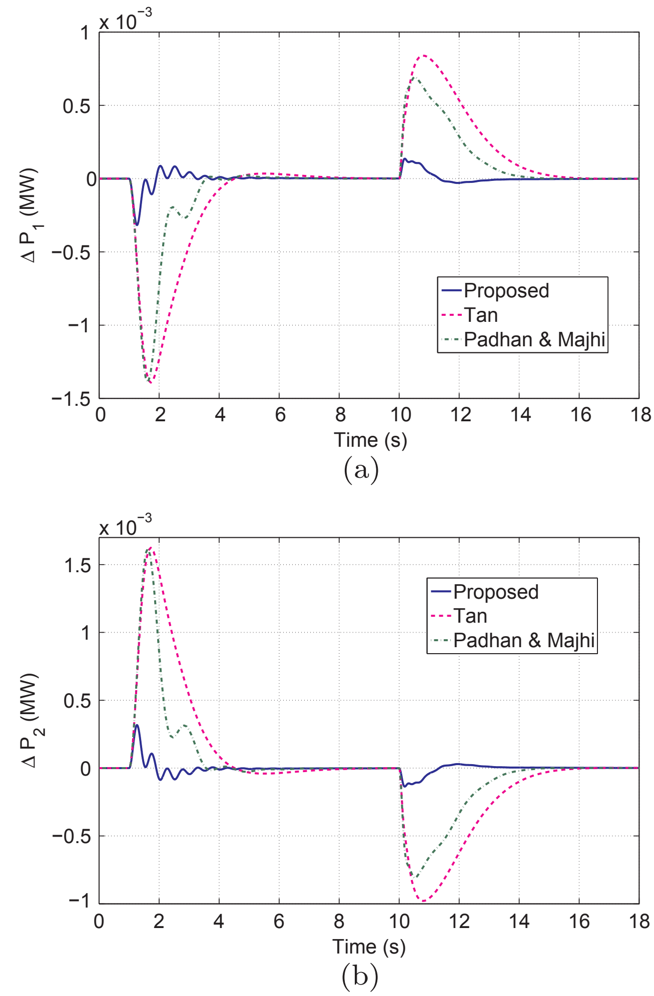

Fig. 8. Tie-line power deviation for (a) area 1 and (b) area 2.

The plant model without droop characteristics is

$$P(s) = \frac{-4s + 1}{(0.2s + 1)(2s + 1)(6s + 1)} \tag{57}$$

Eq. (57) can be factorized in non-minimum phase part: $P_+(s) = -4s + 1$ and

$$P_-(s) = \frac{1}{(0.2s + 1)(2s + 1)(6s + 1)}. \tag{58}$$

Using (40), the reduced-model concept is applied to $\overline{P}_-(s)$ which gives

$$\overline{P}_-(s) = \frac{8.2}{111.52s^2 + 67.24s + 8.2} \tag{59}$$

Using the specification $\omega_{gc} = 0.09$ rad/s and $\phi_m = \pi/4$, the proposed controller becomes

$$C_2(s) = 0.0635\left(8.2 + \frac{1}{s} + 13.6s\right)\left(\frac{1}{s^{0.5}}\right) \tag{60}$$

The proposed controllers are applied to the actual LFC system having reheated and hydro turbines in area 1 and area 2, respectively. The responses of frequency and tie-line power deviation of step load of $\Delta P_{d,i} = 0.01$ $(i = 1, 2)$ occurring at $t = 1$ s and $t = 30$ s, respectively, in area 1 and 2, are presented in Figs. 9 and 10, which shows that the fluctuations in frequency and tie-line power tend to zero.

6.4. LFC design in presence of GRC and GDB

We consider a more realistic condition of power system where the physical constraints such as generation rate constraint (GRC) in turbine and governor dead band (GDB) exist (see Fig. 11). To test the utility of the proposed controller, the study is extended to the case described in Section 5.1. A generation rate limitation of 0.1 p.u. per minute is considered here, *i.e.*, $\Delta P_G \leqslant 0.1$ p. u. /min = 0.0017 p. u. /s [37] and the GDB width considered is 0.036 Hz [40]. Using the specification

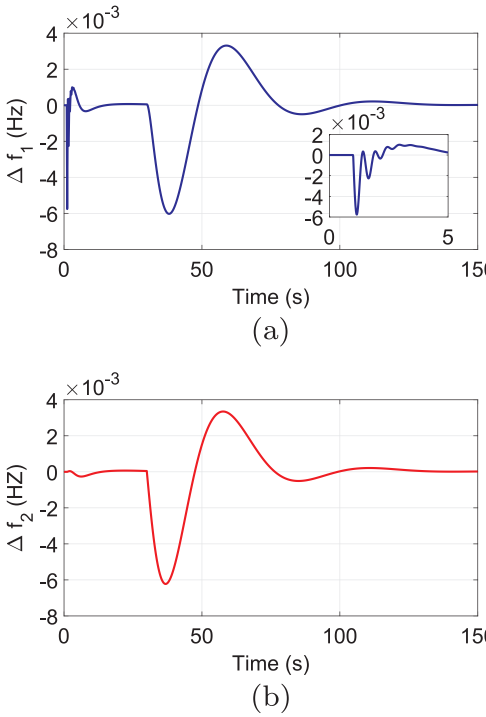

Fig. 9. Frequency deviation for (a) area 1 (reheated turbine) and (b) area 2 (hydro turbine).

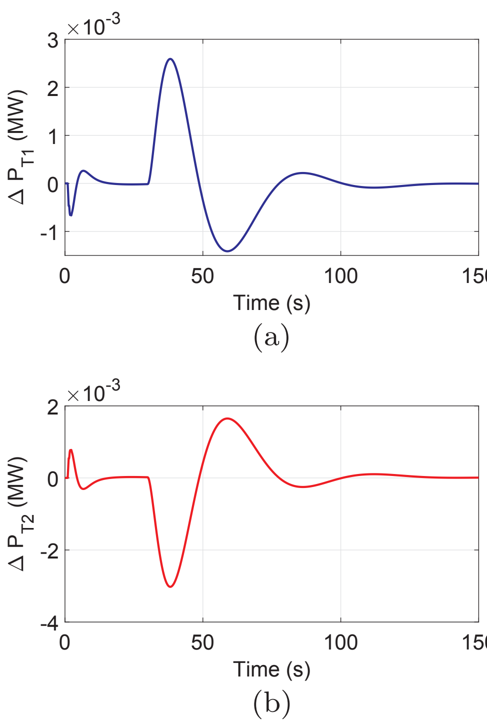

Fig. 10. Tie-line power deviation for (a) area 1 (reheated turbine) and (b) area 2 (hydro turbine).

$\omega_{gc} = 0.01$ rad/s and $\phi_m = \pi/4$, the proposed scheme yields

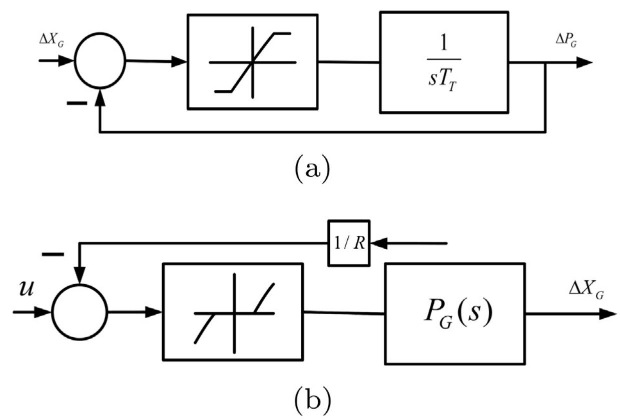

Fig. 11. (a) Turbine model with GRC and (b) dead-band in governor control loop.

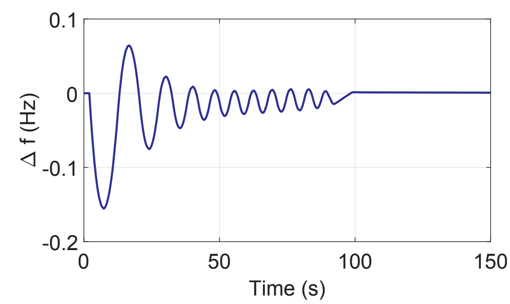

Fig. 12. Response in presence of GRC and GDB.

$$C(s) = 1.726 \times 10^{-4}\left(1 + \frac{2.5026}{s} + 0.3146s\right)\left(\frac{1}{s^{0.5}}\right) \tag{61}$$

The response of the frequency deviation is depicted in Fig. 12 which shows that the proposed scheme can also work well in presence of GRC and GDB constraints.

7. Conclusion and future work

This paper proposes a simple analytical PID load-frequency controller to improve power system performance via fractional-order IMC tuning and reduced-order modeling scheme. The computer simulations have been conducted for single and multi-area power systems consisting different types of turbines and physical limitations. The proposed scheme brings good disturbance rejection and eliminates modeling error and parametric uncertainties.

The merits of the proposed scheme can be accounted in terms of simplicity in the design algorithm because the conventional fractional-order control schemes require complex mathematical manipulations or optimization techniques to evaluate the tuning parameters. The other advantage is that the controller evolved through the design process is PID controller followed by a fractional-order integrator. As far as LFC is concerned, this paper will serve a valuable resource for further research when other physical constraints such as crossover elements in a thermal unit and communication delays are present in power systems. Moreover, this work will encourage the researchers to investigate the efficient reduced-order modeling algorithms for better dynamic performance of power systems.

Appendix A. Asymptotic behavior of $T(j\omega)$

Eq. (18) can be rewritten as

$$\begin{aligned}|T(\mathrm{j}\omega)|_{\mathrm{dB}} &= 20\log\frac{1}{\sqrt{1+2\tau\omega^{\gamma}\cos\frac{\gamma\pi}{2}+(\tau\omega^{\gamma})^2}}\\ &= \frac{1}{2}\times 20\log\frac{1}{1+2\tau\omega^{\gamma}\cos\frac{\gamma\pi}{2}+(\tau\omega^{\gamma})^2}\\ &= -10\log\left(1+2\tau\omega^{\gamma}\cos\frac{\gamma\pi}{2}+(\tau\omega^{\gamma})^2\right)\\ &= -10\log\left((\tau\omega^{\gamma})^2\left[\frac{1}{(\tau\omega^{\gamma})^2}+2\frac{\cos\frac{\gamma\pi}{2}}{\tau\omega^{\gamma}}+1\right]\right)\\ &= -20\log\left((\tau\omega^{\gamma})\left[\frac{1}{(\tau\omega^{\gamma})^2}+2\frac{\cos\frac{\gamma\pi}{2}}{\tau\omega^{\gamma}}+1\right]\right)\end{aligned} \tag{A.1}$$

Therefore, the asymptotic behavior of (A.1) is obtained as

$$\lim_{\omega\to\infty}|T(\mathrm{j}\omega)|_{\mathrm{dB}} \approx -20\gamma\log(\tau\omega)$$

Similarly (19) can be produced as

$$\begin{aligned}\arg[T(\mathrm{j}\omega)] &= -\arctan\left[\frac{\tau\omega^{\gamma}\sin\frac{\gamma\pi}{2}}{1+\tau\omega^{\gamma}\cos\frac{\gamma\pi}{2}}\right]\\ &= -\arctan\left[\frac{\sin\frac{\gamma\pi}{2}}{\frac{1}{\tau\omega^{\gamma}}+\cos\frac{\gamma\pi}{2}}\right]\end{aligned} \tag{A.2}$$

and therefore for (A.2), we have

$$\lim_{\omega\to\infty}\arg[T(\mathrm{j}\omega)] \approx -\frac{\gamma\pi}{2}$$

Appendix B. Derivation of ω_r and M_r

From Definition 4, $M_r = \max |T(\mathrm{j}\omega)|_{\omega=\omega_r}$ and it is maximum when the denominator term of (17), *i.e.*,

$$d(\omega) = \left(1+\tau\omega^{\gamma}\cos\frac{\gamma\pi}{2}\right)+\mathrm{j}\tau\omega^{\gamma}\sin\frac{\gamma\pi}{2} \tag{B.1}$$

is minimum. Now differentiate (B.1) with respect to ω, and equate to zero, *i.e.*,

$$\frac{\mathrm{d}}{\mathrm{d}\omega}\left[\left(1+\tau\omega^{\gamma}\cos\frac{\gamma\pi}{2}\right)+\mathrm{j}\tau\omega^{\gamma}\sin\frac{\gamma\pi}{2}\right]=0$$

we get $\omega_r = \frac{1}{\tau}\left|\cos\frac{\gamma\pi}{2}\right|^{frac1\tau}$. On substituting ω_r in (18), we get $M_r = \frac{1}{\sin\frac{\gamma\pi}{2}}$.

Appendix C. Derivation of ω_p and ζ

From (16), the characteristic equation is

$$1+\tau s^{\gamma}=0$$

The two poles are given by $s_{1,2} = \frac{1}{\tau}e^{\pm\mathrm{j}\frac{\pi}{\gamma}}$. The poles are complex and conjugate and form a center angle 2θ with respect to imaginary $\mathrm{j}\omega$ axis, where $\theta = \pi\left(1-\frac{1}{\gamma}\right)$. Now, from the information of the poles, *i.e.*, through the modulus $\frac{1}{\tau}$ and θ, we can obtain

$$\omega_p = \frac{1}{\tau}\sin\theta = \frac{1}{\tau}\sin\pi\left(1-\frac{1}{\gamma}\right) = \frac{1}{\tau}\sin\frac{\pi}{\gamma}$$

and

$$\zeta = \cos\theta = \cos\pi\left(1-\frac{1}{\gamma}\right) = -\cos\frac{\pi}{\gamma}$$

Appendix D. Integer-order approximation of FO transfer function

In simulation, the Oustaloup method [39] is used to find integer-order approximations of FO transfer function in which

$$s^{\mu} = K\prod_{i=1}^{N}\frac{s+\widetilde{\omega}_i}{s+\omega_i} \tag{D.1}$$

where $\widetilde{\omega}_i = \omega_l\omega_r^{(2i-1-\alpha)/N}$, $\omega_i = \omega_l\omega_r^{(2i-1+\alpha)/N}$, $K=\omega_h^{\alpha}$ and $\omega_r = \sqrt{\frac{\omega_h}{\omega_l}}$. Note that the number of poles and zeros (N) of approximating transfer function and the frequency range ($[\omega_l, \omega_h]$) must be selected before evaluating (D.1). When $\mu > 1$ then it can be written in the form $s^{\mu} = s^{[\mu]}s^{\delta}$ where $[\mu]$ is greatest integer and then the term s^{δ} is replaced by approximation transfer function (D.1).

Appendix E. Supplementary data

Supplementary data associated with this article can be found, in the online version, at https://doi.org/10.1016/j.ijepes.2018.07.005.

References

[1] Kundur P, et al. Definition and classification of power system stability IEEE/CIGRE joint task force on stability terms and definitions. IEEE Trans. Power Syst. 2004;19(3):1387–401.
[2] Bevrani H. Robust power system frequency control. Springer; 2009.
[3] Saxena S, Hote YV. Load frequency control in power systems via internal model control scheme and model-order reduction. IEEE Trans. Power Syst. 2013;28(3):2749–57.
[4] Saxena S, Hote YV. Decentralized PID load frequency control for perturbed multi-area power systems. Int. J. Electric Power Energy Syst. 2016;81:405–15.
[5] Ibraheem Kumar P, Kothari DP. Recent philosophies of automatic generation control strategies in power systems. IEEE Trans. Power Syst. 2005;20(1):346–57.
[6] Shayeghi H, Shayanfar HA, Jalili A. Load frequency control strategies: a state-of-the-art survey for the researcher. Energy Convers. Manage. 2009;50:344–53.
[7] Pandey SK, Mohanty SR, Kishor N. A literature survey on load-frequency control for conventional and distribution generation power systems. Renew. Sustain. Energy Rev. 2013;25:318–34.
[8] Padula F, Visioli A. Advances in robust fractional control. Springer; 2015.
[9] Monje CA, Chen YQ, Vinagre BM, Xue D, Feliu V. Fractional-order systems and controls: fundamentals and applications. Springer; 2010.
[10] Alomoush MI. Load frequency control and automatic generation control using fractional-order controllers. Electr. Eng. 2010;91:357–68.
[11] Sondhi S, Hote YV. Fractional order PID controller for load frequency control. Energy Convers. Manage. 2014;85:343–53.
[12] Debbarma S, Saikia LC, Sinha N. Automatic generation control using two degree of freedom fractional order PID controller. Int. J. Electr. Power Energy Syst. 2014;58:120–9.
[13] Pan I, Das S. Fractional-order load-frequency control of interconnected power systems using chaotic multi-objective optimization. Appl. Soft Comput. 2015;29:328–44.
[14] Taher SA, Fini MH, Aliabadi SF. Fractional order PID controller design for LFC in electric power systems using imperialist competitive algorithm. Ain Shams Eng. J. 2014;5:121–35.
[15] Morari M, Zafiriou E. Robust process control. NJ, Prentice-Hall: Englewood Cliffs; 1989.
[16] Saxena S, Hote YV. Advances in internal model control technique: a review and future prospects. IETE Tech. Rev. 2012;29(6):461–72.
[17] Gaona DC, Goytia ELM, Lara OA. Fault ride-through improvement of DFIG-WT by integrating a two-degrees-of-freedom internal model control. IEEE Trans. Industr. Electron. 2013;60(3):1133–45.
[18] Yazdanian M, Sani AM. Internal model-based current control of the RL filter-based voltage-sourced converter. IEEE Trans. Energy Convers. 2014;29(4):873–81.
[19] Saxena S, Hote YV. Simple approach to design PID controller via internal model control. Arab. J. Sci. Eng. 2016;41(9):3473–89.
[20] Saxena S, Hote YV. Internal model control based PID tuning using first-order filter. Int J Control Autom Syst (in press).
[21] Muresana CI, et al. Tuning algorithms for fractional order internal model controllers for time delay processes. Int. J. Control 2016;89(3):579–93.
[22] Lanusse P, Malti R, Melchior P. CRONE control system design toolbox for the control engineering community: tutorial and case study. Philos. Trans. R. Soc. A 2013;371.
[23] Maâmar B, Rachid M. IMC-PID-fractional-order filter controller design for integer order systems. ISA Trans. 2014;53:1620–8.
[24] Podlubny I. Fractional differential equations. San Diego: Academic Press; 1999.
[25] Fortuna L, Nunnari G, Gallo A. Model order reduction techniques with applications in electrical engineering. London: Springer-Verlag; 1992.
[26] Benner P, Mehrmann V, Sorensen DC. Dimension reduction of large-scale systems. Springer; 2005.
[27] Schilders WH, Van der Vorst HA, Rommes J. Model order reduction: theory, research aspects and applications. Springer; 2008.
[28] Fortuna L, Frasca M. Optimal and robust control: advanced topics with MATLAB. CRC Press; 2012.
[29] Hutton MF, Friedland B. Routh approximations for reducing order of linear, time-invariant systems. IEEE Trans. Autom. Control 1975;AC-20:329–37.
[30] Oustaloup A. La commande CRONE. Paris: Hermès Editions; 1991.
[31] Sabatier J, et al. CRONE Control: principles and extension to time-variant plants with asymptotically constant coefficients. Nonlinear Dyn. 2002;29:363–85.
[32] Malti R, Moreau X, Khemane F, Oustaloup A. Stability and resonance conditions of elementary fractional transfer functions. Automatica 2011;47(11):2462–7.
[33] Kundur P. Power systems stability and control. Mc-Graw Hill; 1994.
[34] Tan W. Load frequency control: problems and solutions. In: Proc. 30th Chinese Control Conference, Yantai, China, July 22–24; 2011.
[35] Tan W. Unified tuning of PID load frequency controller for power systems via IMC. IEEE Trans. Power Syst. 2010;25(1):341–50.
[36] Anwar MN, Pan S. A new PID load frequency controller design method in frequency domain through direct synthesis approach. Electr. Power Energy Syst. 2015;67:560–9.
[37] Tan W. Tuning of PID load frequency controller for power systems. Energy Convers. Manage. 2009;50:1465–72.
[38] Padhan DG, Majhi S. A new control scheme for PID load frequency controller of single-area and multi area power systems. ISA Trans. 2013;52:242–51.
[39] Oustaloup A, Levron F, Mathieu B, Nanot FM. Frequency band complex noninteger differentiator: characterization and synthesis. IEEE Trans. Circuits Syst. I: Fundam. Theory Appl. 2000;47(1):25–39.
[40] IEEE Standard 122-1991. Recommended practice for functional and performance characteristics of control systems for steam turbine-generator units; 1992.